INTERNATIONAL JOURNAL OF HEALTH & MEDICAL RESEARCH

ISSN(print): 2833-213X, ISSN(online): 2833-2148

Volume 02 Issue 09 September 2023

DOI : 10.58806/ijhmr.2023.v2i9n07

Page No. 296-303

Spatial Patterns of Hand-Foot and Mouth Disease In Ho Chi Minh City, Vietnam

Thi-Quynh Nguyen[1,*], Thi-Bich-Thuy Luong[1], Thi-Thuy Ngo[2], Thi-Yen Mai[3]

[1] Faculty of Nursing, East Asia University of Technology, Hanoi, Vietnam

[2] Faculty of Nursing, Phenikaa University, Hanoi, Vietnam

[3] Preclinical Research Center, Nam Dinh University of Nursing, Nam Dinh, Vietnam

ABSTRACT:

Background: Hand-Foot-and-Mouth Disease (HFMD) is most frequently caused by Enterovirus71 (EV-A71) or Coxsackie virus A16 (CV-A16), infants and young children are at greatest risk. Describing the spatial patterns of HFMD can help develop and better target interventions. The objective of this study is to identify spatial patterns of HFMD in the first 8-months of 2023 in Ho Chi Minh city, Vietnam. **Methods:** The global Moran's I statistic, Moran's I scatterplot and local Moran's I statistic and Boxplot will be applied to study spatial patterns of HFMD. Spatial patterns including spatial clusters (high-high and low-low) and spatial outliers (low-high and high-low) will be identified for HFMD cases and HFMD infection rates. **Results:** three high-high spatial clusters were mainly distributed in districts in the western region of the city such as Binh Tan, Binh Chanh, and Tan Phu. These high-high spatial clusters belonged to districts having the highest rates of HFMD infections in the city with their corresponding rates of 289, 283 and 281 cases/100,000 inhabitants, respectively. On the other hand, two low-low spatial clusters were detected in Districts 1 and 5 in the city center with their HFMD infection rates of 190 and 209 cases/100,000 inhabitants, respectively. **Conclusions :** findings in this study support the usefulness of boxplots, local and global Moran's I statistics, and Moran's I scatterplots in the identification of spatial clusters and spatial outliers of HFMD.

KEYWORDS: Spatial Patterns, Hand-Foot-and-Mouth Disease, Local Moran's I, Ho Chi Minh city, Vietnam.

1. INTRODUCTION

As early as 1957, the characteristic symptoms of fever, vesicular rash on hands and feet caused by Coxsackievirus (CV), primarily CVA16, was first reported in Toronto (1,2). In 1959, "hand-foot-and-mouth disease (HFMD)" was initially used to name a disease. HFMD is a viral illness commonly seen in young children under 5 years of age, characterized by typical manifestations such as oral herpes and rashes on the hands and feet (3). Over the past few decades, HFMD outbreaks caused by Enterovirus A71 (EV-A71), CVA16, CVA6 and Echoviruses (Echo) were reported frequently around the world (4). HFMD is caused by Human enteroviruses (EVs) that are members of the Enterovirus genus of the Picornaviridae family (5). EVs were initially classified into Poliovirus (PV), Echo, CV-A and B, and emerging EVs. Since 1999, EVs have been divided into four categories of Enterovirus A, B, C, and D, in the light of their molecular, biological, and genetic characteristics (3). The HFMD disease was generally mild and lasted less than a week in most cases, characterized by fever, a blister-like rash on the hands and feet, and oral ulcers caused by ruptured blisters in the mouth (6). Therefore, HFMD has become a significant concern for public health throughout the Asia-Pacific region including Vietnam and beyond (3).

HFMD-related data relates to geographical locations which have a spatial and geographic dimension and can be considered a type of spatial object. Such epidemiological data as HFMD can be studied using spatial statistics (7). Spatial statistic is an essential tool to examine the spatial pattern of spatial objects (8). Following this idea of Tobler's First Law of Geography, widely used statistics for spatial auto-correlation analysis such as global spatial statistics (Moran's I, Getis-Ord G* and Geary's C) and local indicators of spatial association (LISA) have been successfully employed in epidemiological studies (9–12) in general, and in the study of the spread of COVID-19 (13–15) and HFMD (16,17) in particular. For example, a study on spatiotemporal analysis and hotspots detection of COVID-19 in southern, northern and western Europe was carried out using spatial statistics (18). Local Moran's I autocorrelation coefficient, Getis-Ord General-G high/low clustering, and Getis-Ord Getis-Ord's G_i^* statistic were emloyed to study spatio-temporal COVID-19 spread over Oman (19). For HFMD studies, a lots of attempts have been put into the use of spatial statistics in studies of the spread of HFMD. For instance, spatio-temporal distribution and hotspots of HFMD were successfully carried out in in northern Thailand (20). Spatial clustering and changing trend of hand-foot-mouth disease were identified during 2008-2011 in China (21). GIS has been also used to map HFMD reported cases for the whole of Sarawak. In that study, thematic

Map of HFMD based on division was later produced (22). In 2014, a study has been conducted for a temporal and spatial mapping of HFMD that covered 13 all divisions of Sarawak. This study focused on reported cased of HFMD from the year 2006 until 2012. It wasfound that there was no significant clustering was detected (23). Subsequently in the year 2016, with the objective to identify the spatial spreading pattern of HFMD for urban divisions and non-urban Inverse Distance Weighted was used to interpolate the reported HFMD cases for the whole of Sarawak to identify the high-risk pattern of HFDM (24).

The aim of this study is to investigate the spatial patterns of HFMD the first 8 months of 2023 in Ho Chi Minh city, Vietnam. The global Moran's I statistic, Moran's I scatterplot and local Moran's I statistic and Boxplot will be applied to study spatial patterns of HFMD. Spatial patterns including spatial clusters (high-high and low-low) and spatial outliers (low-high and high-low) will be identified for HFMD cases and HFMD infection rates in Ho Chi Minh city.

2. MATERIALS AND METHODS

2.1. Materials and study area

Since the beginning of 2023, certain districts in the city have witnessed a high incidence rate of HFMD infections per 100,000 people such as Binh Tan, Binh Chanh, Tan Phu, District 6, and District 8 (25). According to Ho Chi Minh City's health sector, the HFMD epidemic has increased rapidly and may last another 3-4 months since August, 2023. In particular, the time students returning to school will coincide with the second peak of the HFMD epidemic. In the most recent week (week 27th), the city recorded 1,614 HFMD cases, showing an alarming increase of almost 2.5 times compared to the average of 716 cases reported four weeks earlier (25). HFMD has emerged in Vietnam since 2003 in which Ho Chi Minh City is particularly a southern city with the highest cases and mortality numbers of HFMD in the whole country (26). Therefore, analysis of spatial patterns of HFMD in the city plays an important role in the control of the disease. Data used in this study were collected in Ho Chi Minh City during the first 8 months of 2023.

2.2. Methods

This study used the global Moran's I statistic to determine where the HFMD was spatially clustered on a global scale (27,28). The definition of the global Moran's I statistic is expressed in equation (1):

$$I = \frac{n}{S_0}\frac{\sum_{i=1}^{n}\sum_{j=1}^{n} W_{ij}(x_i - \bar{x})(x_j - \bar{x})}{\sum_{i=1}^{n}\sum_{j=i}^{n} W_{ij}\sum_{i=1}^{n}(x_i - \bar{x})^2} \quad (1)$$

where x_i and x_j are the HFMD for districts i and j; $\bar{x}$ is the mean of the HFMD and be given by $\bar{x} = \sum_{i=1}^{n}\frac{x_i}{n}$; n is the total number of districts in the whole study area; and W_{ij} is a $(n \times n)$ spatial weight matrix (29).

The interval [-1, +1] contains the values of the global Moran's I coefficient. (29). Positive values of Moran's I result from the data's positive spatial autocorrelation, whereas Moran's I values are negative when there is a negative spatial autocorrelation (30). Global Moran's I coefficient values close to zero demonstrate that there is no geographical autocorrelation or randomness in the HFMD distribution.

The overall existence or absence of spatial autocorrelation is reflected by the global Moran's I. The regional Moran's I statistic was used to quantify the spatial clustering of low and high number of HFMD in each district (29). The local Moran's I statistic (I_i) of HFMD at district i is given by the following equation (31):

$$I_i = \frac{(x_i - \bar{x})}{\sigma^2}\sum_{j\#i, j\in J_i}^{N} W_{ij}(x_j - \bar{x}) \quad (2)$$

where x_i, x_j, $\bar{x}$, and W_{ij} are defined in equation (1); N is the total number of neighborhood districts (29); J_i denotes the neighborhood set of HFMD at district i; j#i implies that the sum of all $(x_j - \bar{x})$ of nearby neighbourhood districts of district i but not including x_j; and σ^2 is the variance of x, given in equation (3). In this study, W_{ij} defines neighbor connectivity and is constructed using first order of contiguity.

$$\sigma^2 = \frac{1}{N}\sum_{j=1}^{N}(x_i - \bar{x}) \quad (3)$$

Local Moran's I statistics show the degree of spatial clustering of HFMD in each district. Similar to the global Moran's I statistic, the local Moran's I value at district i (I_i) also ranges between -1 and +1. There is no spatial autocorrelation of HFMD if the local Moran's I coefficient at district i equals zero ($I_i = 0$). If $I_i > 0$ then there will be a positive spatial autocorrelation of HFMD (29). If $I_i < 0$ then there will be a negative spatial autocorrelation of HFMD. A high positive I_i shows the district i has a similarly high or low number of HFMD cases as its neighbors and called the ''spatial cluster''(30) (Figure 1). In this case, when there is a positive local spatial autocorrelation, the local Moran's I statistic indicates two types of spatial clusters for HFMD cases, including: high-high spatial clusters and low-low spatial clusters. Low-high and high-low clusters are also two forms of spatial outliers that are identified using the local Moran's I statistic when there is a negative local spatial autocorrelation (Figure 1).

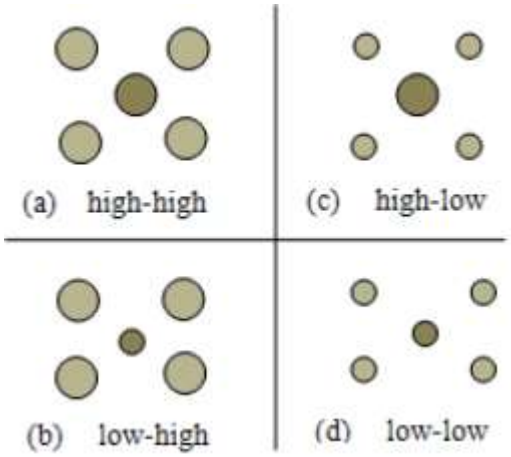

Figure 1. Spatial clusters and spatial outliers.

The statistical significance of Moran's I statistic can be tested if I_i follows the normal distribution, the Z-scores can be determined as follows:

$$Z_{I_i} = -\frac{I_i - E(I_i)}{\sqrt{Var(I_i)}} \quad (4)$$

where: $E(I_i)$ and $Var(I_i)$ are the arithmetic expectation and variance of the Moran statistic at district i, respectively, and are expressed using by the following equations::

$$E(I_i) = -\frac{w_i}{n-1} \quad (5)$$

$$Var(I_i) = E(I_i^2) - [E(I_i)]^2 = \frac{w_{i(2)}(n-b_2)}{n-1} + \frac{2w_{i(kh)}(2b_2-n)}{(n-1)(n-2)} + \frac{{w_i}^2}{(n-1)^2} \quad (6)$$

with:

$$E(I_i) = -\frac{w_i}{n-1} \quad (5)$$

$$Var(I_i) = E(I_i^2) - [E(I_i)]^2 = \frac{w_{i(2)}(n-b_2)}{n-1} + \frac{2w_{i(kh)}(2b_2-n)}{(n-1)(n-2)} + \frac{{w_i}^2}{(n-1)^2} \quad (6)$$

$$w_i = \sum_{j=1}^{n} w_{ij}(d) \quad (7)$$

$$b_2 = \left[\frac{1}{n}\sum_{i=1}^{n}(x_i - \bar{x})^4\right]\left[\frac{1}{n}\sum_{i=1}^{n}(x_i - \bar{x})^2\right]^{-2} \quad (8)$$

$$w_{i(2)} = \sum_{j=1}^{n} w_{ij}(d)^2 \quad (9)$$

$$2w_{i(kh)} = \sum_{\substack{k=1 \\ k\neq i}}^{n}\sum_{\substack{h=1 \\ h\neq i}}^{n} w_{ik}(d)w_{ih}(d) \quad (10)$$

With the help of the spatial statistics software, GeoDA, developed by (32), a randomization test with 999 permutations was used in this work to testing for the significance spatial autocorrelation statistics. A total of 999 permutations were used to create and test spatial autocorrelation statistics at the significance level of 0.05.

3. RESULTS AND DISCUSSIONS

3.1. Analysis of distribution of HFMD

The histogram and map of HFMD per 100,000 population were shown in Figure 2. Data from Figure 2 (left) demonstrate that the distribution of HFMD cases per 100,000 population for each district. In the first 8 months of 2023, five districts having the high HFMD infection rates included Binh Tan (289 cases/100,000 people), Binh Chanh (283 cases/100,000 inhabitants), Tan Phu (281 cases/100,000 inhabitants), Nha Be (272 cases/100,000 inhabitants) and District 12 (264 cases/100,000 inhabitants). Meanwhile, five districts having low HFMD infection rates included Can Gio (152 cases/100,000 inhabitants), Cu Chi (158 cases/100,000 inhabitants), Phu Nhuan (163 cases/100,000 inhabitants), District 3 and 4 with 181 cases/100,000 inhabitants. Data from the pecentile map in Figure 1 (right) illustrate that districts having high HFMD infection rates were mainly concentrated in the central and western and southwest areas of Ho Chi Minh city. The latest data shows that, from August 14, 2023 to August 20, 2023, a total

of 1,869 HFMD cases was reported. The number of HFMD have decreased. In this period, districts with a high number of cases per 100,000 inhabitants include Binh Tan, Binh Chanh and Tan Phu. Districts having low HFMD infection rates were mainly distributed in the north, east and south areas of the city. Meanwhile, districts having medium HFMD infection rates were mainly distributed in the administrative center of the city.

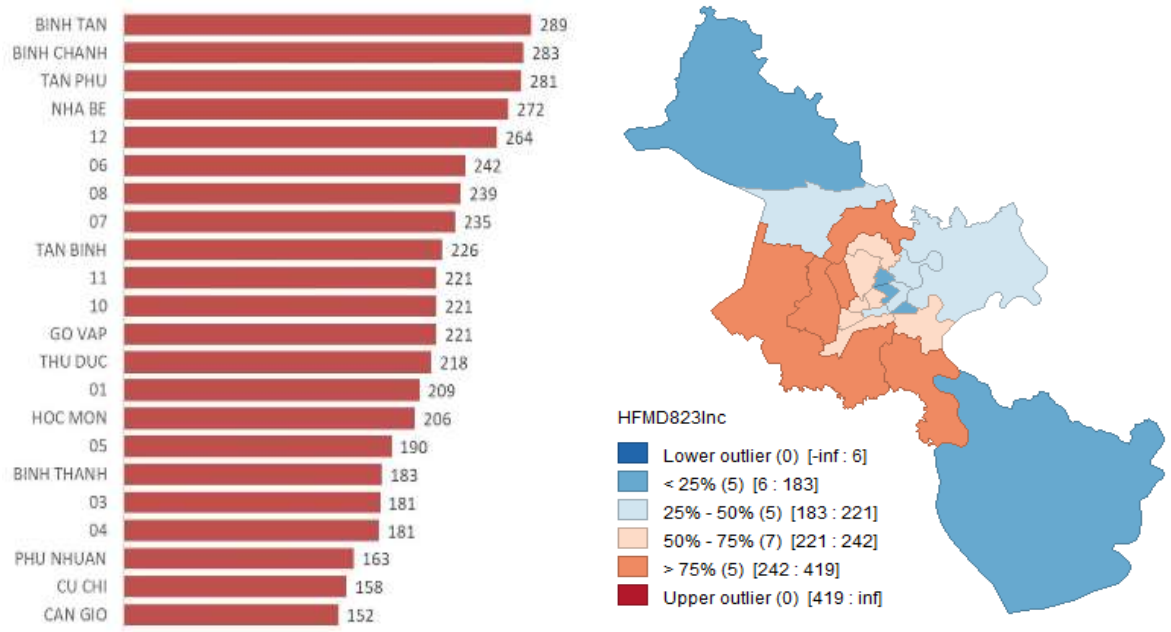

Figure 2. Histogram (left) and map of HFMD distribution in Ho Chi Minh city, Vietnam.

Summary of statistical descriptives on HFMD cases and infection rates are shown in Table 1. Data from Table 1 illustrate that, for the variable of HFMD cases, the minimum (Min), maximum (Max), mean (Mean) and median (Median) values were 152, 289, 200, and 221 cases, respectively. Meanwhile, the interquartile range (IQR) and standard deviation (SDEV) were 59 and 41 cases, respectively. For the variable of HFMD infection rates, the minimum, maximum, mean and median values were 113, 2376, 942, and 793 (cases per 100.000 inhabitants), respectively. Meanwhile, the interquartile range and standard deviation were 877 and 603 (cases per 100.000 inhabitants), respectively. Data from Boxplots in Figure 3 illustrates the distribution of HFMD cases and infection rates. Data in Figure 3 demonstrate the distribution of data is even on both sides. In particular, the distribution of HFMD infection rates was more balanced than that of HFMD infection rates.

Table 1. Summary table of statistical descriptives for HFMD in Ho Chi Minh city.

Statistical descriptives	Min	Mean	Median	Max	Q1	Q3	IQR	SDEV
HFMD cases	152	200	221	289	183	242	59	41
HFMD infection rates	113	942	793	2376	428	1305	877	603

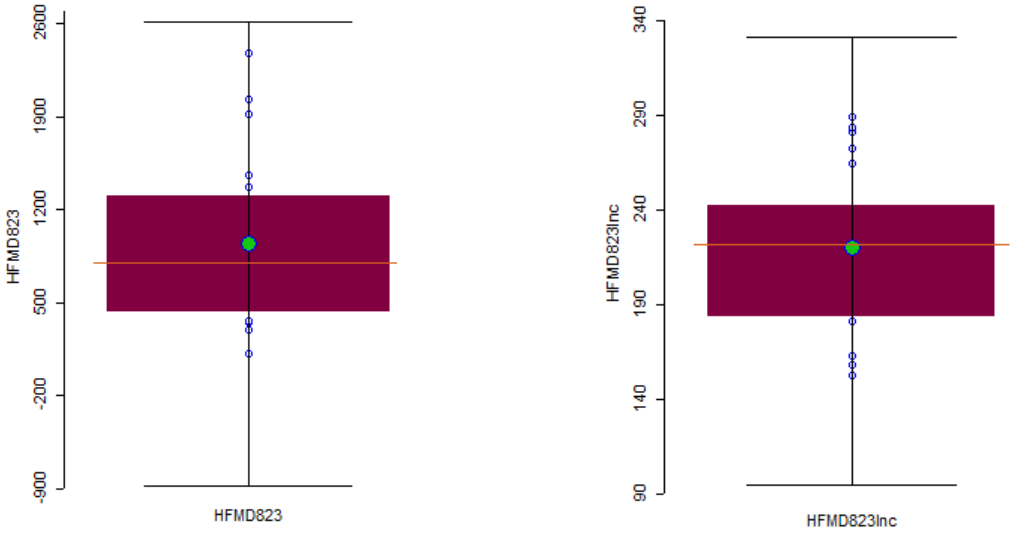

Figure 3. Boxplots of HFMD cases (left) and HFMD incidence (right).

3.2. Analysis of global spatial patterns of HFMD

The global spatial patterns of HFMD are shown by the Moran scatterplots as shown in Figure 3. Data from the Moran scatterplot illustrates that global Moran's statistics for HFMD cases and HFMD infection rates were 0.17 and 0.195, respectively. The coefficients of global Moran's I statistic were greater than 0 indicating that, overall, there existed a positive spatial correlation in the city. Positive spatial autocorrelation means that geographically nearby values of a variable tend to be similar on a map: high number of HFMD cases tend to be located near high number of HFMD cases, medium values near medium values, and low values near low values. It can be seen from Figure 4 that the Moran's scatter plot on the right has a higher degree of dispersion than those on the left.

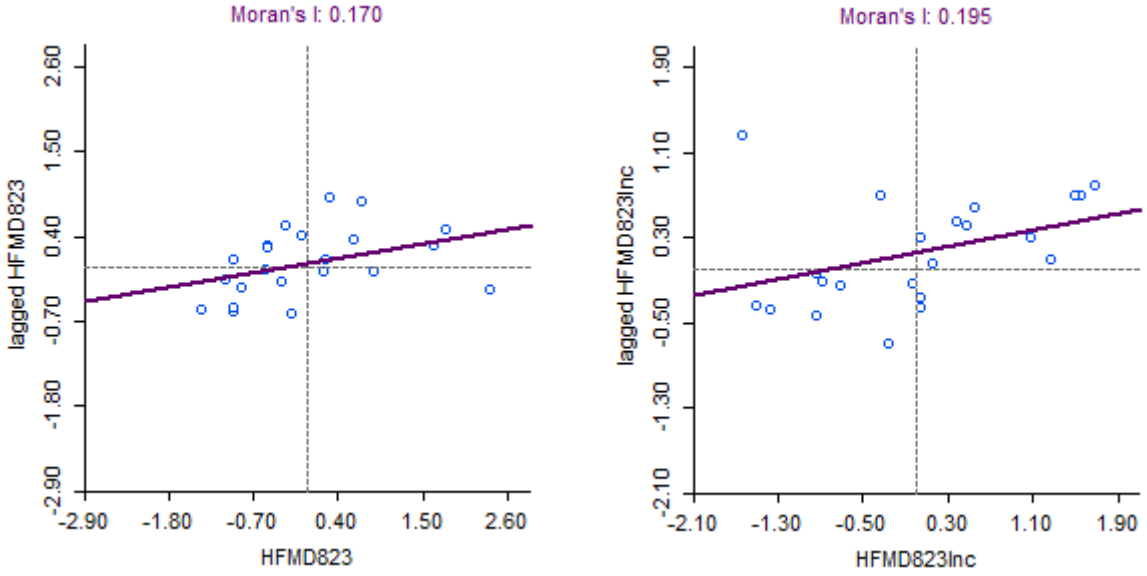

Figure 4. Moran's I scatterplots of HFMD cases (left) and HFMD incidence (right).

3.3. Analysis of local spatial patterns of HFMD

Statistical descriptives of LISA clusters are summarized in Table 2. Data from Table 2 illustrate that, in the case of using data on HFMD cases, the minimum, maximum, mean and median values of LISA were -0.68, 0.16, 0.09 and 0.88, respectively. Meanwhile, the interquartile range and standard deviation were 0.53 and 0.36, respectively. In case of using data on HFMD infection rates, the minimum, maximum, mean and median values of LISA were -2.1, 0.19, 0.14, and 1.34, respectively. The corresponding values of interquartile range and standard deviation were 0.4 and 0.64, respectively. Data from Boxplots in Figure 3 illustrates the distribution of HFMD cases and infection rates. Data in Figure 5 (right) demonstrate the distribution of data is more concentrated in the center of the boxplot than those obtained in Figure 5 (left).

Table 2. Summary table of statistical descriptives for LISA in Ho Chi Minh city.

Statistical descriptives	Min	Mean	Median	Max	Q1	Q3	IQR	SDEV
HFMD cases	-0.68	0.16	0.09	0.88	-0.05	0.48	0.53	0.36
HFMD infection rates	-2.1	0.19	0.14	1.34	0.01	0.41	0.4	0.64

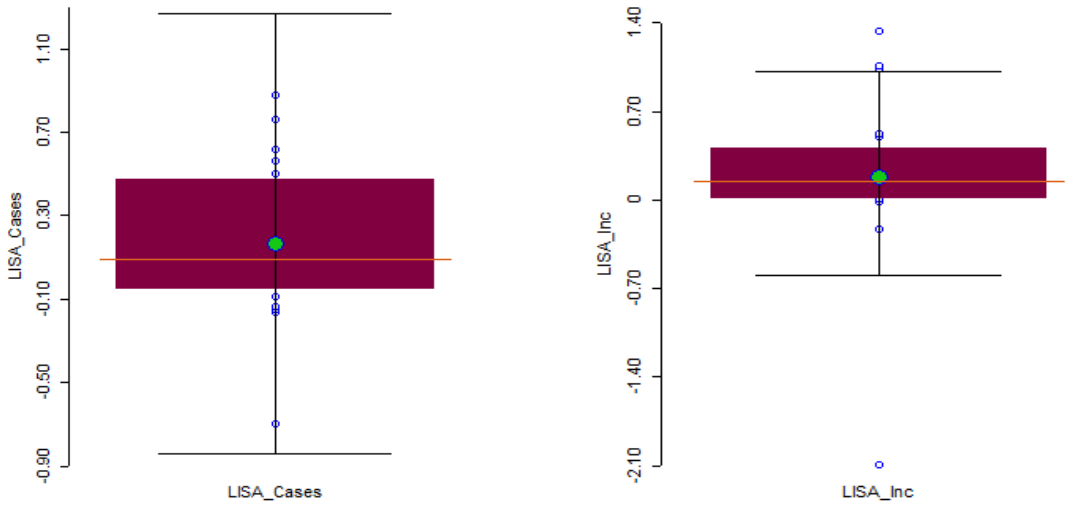

Figure 5. Boxplots of LISA for HFMD cases (left) and HFMD incidence (right).

In the case of using HFMD cases, data from the LISA cluster map in Figure 6 (left) demonstrate that a total of 4 spatial clusters including three high-high and one low-low clusters were successfully detected and 18 districts with unstatistically significance at the level of 0.05. The three high-high spatial clusters were mainly distributed in districts in the northern areas of the city, including Hoc Mon (1117 cases with 283 cases/100,000 inhabitants), District 12 (1373 cases with 2264 cases/100,000 inhabitants), và Binh Tan (2030 cases with 289 cases/100,000 inhabitants). A low-low spatial cluster was identified in District 5 in the city center with only 356 cases and 190 cases/100,000 inhabitants. Similar to those obtained when using data on HFMD cases, in the case of using HFMD infection rates, data from the LISA cluster map in Figure 6 (right) illustrate that a total of 4 spatial clusters including three high-high and one low-low clusters were also successfully detected and 18 districts with unstatistically significance at the level of 0.05. In this case, the three high-high spatial clusters were mainly distributed in districts in the western areas of the city, namely Binh Chanh (283 cases/100,000 inhabitants with 1294 cases), Binh Tan (289 cases/100,000 inhabitants with 2030 cases, and Tan Phu (281 cases/100,000 inhabitants with 1305 cases. A low-low spatial cluster was identified in District 1 in the city center with 209 cases/100,000 inhabitants and 428 cases.

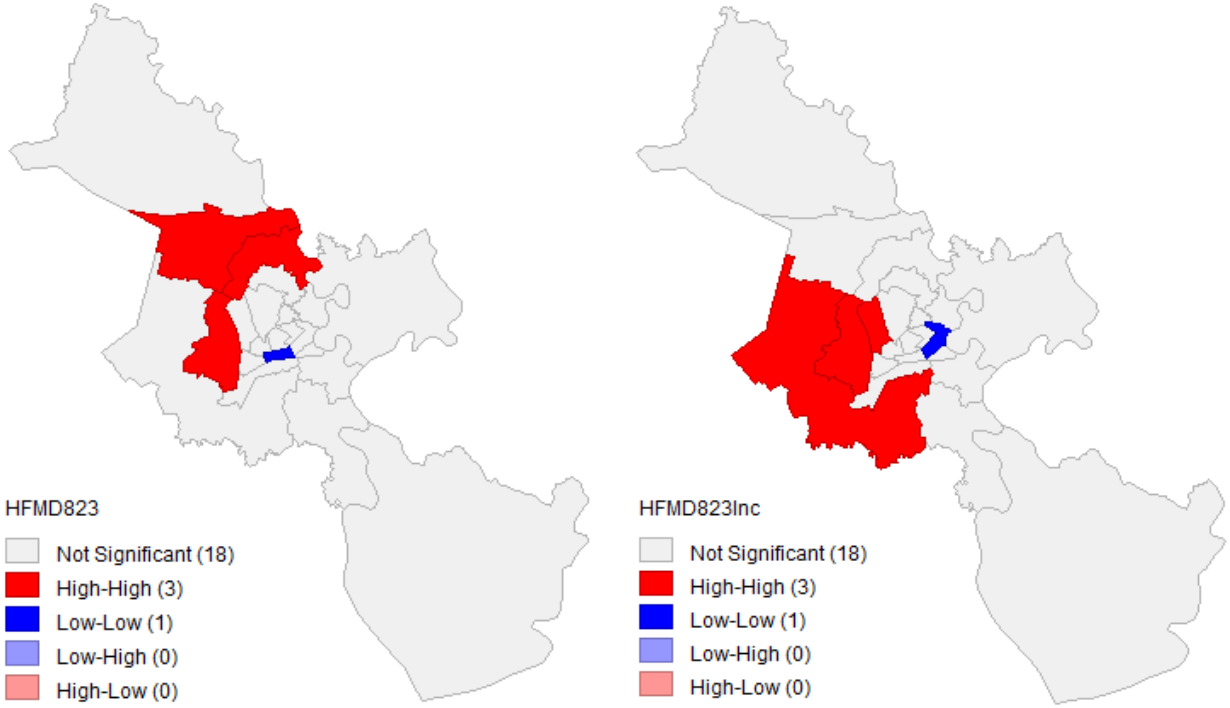

Figure 5. LISA map of HFMD cases (left) and HFMD incidence (right).

According to the above analysis results, three high-high spatial clusters were mainly distributed in districts in the western region of the city such as Binh Tan, Binh Chanh, and Tan Phu. These high-high spatial clusters belong to districts hving the highest rates of HFMD infections in the city with their corresponding rates of 289, 283 and 281 cases/100,000 inhabitants, respectively. On the other hand, two low-low spatial clusters were detected in Districts 1 and 5 in the city center with their HFMD infection rates of 190 and 209 cases/100,000 inhabitants, respectively.

4. CONCLUSIONS

In summary, this objective of this studyis to pinpoint the geographic distribution of HFMD during the first eight months of 2023 in Ho Chi Minh City, Vietnam. The global Moran's I statistic, Moran's I scatterplot and local Moran's I statistic and Boxplot were successfully applied to study spatial patterns of HFMD. Spatial patterns including spatial clusters (high-high and low-low) and spatial outliers (low-high and high-low) were identified for HFMD cases and HFMD infection rates. It was found that the incidence of HFMD was not randomly distributed, with global and local spatial autocorrelations. Three high-high spatial clusters were mainly distributed in districts in the western region of the city such as Binh Tan, Binh Chanh, and Tan Phu. These high-high spatial clusters belonged to districts having the highest rates of HFMD infections in the city with their corresponding rates of 289, 283 and 281 cases/100,000 inhabitants, respectively. On the other hand, two low-low spatial clusters were also detected in Districts 1 and 5 in the city center with their HFMD infection rates of 190 and 209 cases/100,000 inhabitants, respectively. The results of this study confirm the effectiveness of boxplots, local and global Moran's I statistics, and Moran's I scatterplots in the identification of spatial clusters and spatial outliers of HFMD. To develop novel methods for HFMD control, more consideration should be given to the epidemiological and spatiotemporal aspects of the disease. At urban-rural intersections and in kindergartens, health issues should

be highlighted in particular. In addition, new strategies and methods must be developed and more attention paid to the epidemiological and spatiotemporal characteristics of HFMD so that control measures can be improved.

DECLARATION BY AUTHORS

ETHICAL APPROVAL: Approved

ACKNOWLEDGEMENT: The Ho Chi Minh Centre for Disease Control (HCDC), which provided the information, is acknowledged by the authors. The authors thank the editors and the anonymous reviewers for their thoughtful comments and suggestions on this manuscript, which significantly improve the quality of the paper.

SOURCE OF FUNDING: None

CONFLICT OF INTEREST: The authors declare no conflict of interest

REFERENCES

1) Robinson CR, Doane FW, Rhodes AJ. Report of an outbreak of febrile illness with pharyngeal lesions and exanthem: Toronto, summer 1957—isolation of group A coxsackie virus. Can Med Assoc J. 1958;79(8):615.
2) Clarke M, Hunter M, McNAUGHTON GA, Von Seydlitz D, Rhodes AJ. Seasonal aseptic meningitis caused by Coxsackie and ECHO viruses, Toronto, 1957. Can Med Assoc J. 1959;81(1):5.
3) Zhu P, Ji W, Li D, Li Z, Chen Y, Dai B, et al. Current status of hand-foot-and-mouth disease. J Biomed Sci. 2023;30(1):15.
4) Bubba L, Broberg EK, Jasir A, Simmonds P, Harvala H, Redlberger-Fritz M, et al. Circulation of non-polio enteroviruses in 24 EU and EEA countries between 2015 and 2017: a retrospective surveillance study. Lancet Infect Dis. 2020;20(3):350–61.
5) Solomon T, Lewthwaite P, Perera D, Cardosa MJ, McMinn P, Ooi MH. Virology, epidemiology, pathogenesis, and control of enterovirus 71. Lancet Infect Dis. 2010;10(11):778–90.
6) Alsop J, Flewett TH, Foster JR. "Hand-foot-and-mouth disease" in Birmingham in 1959. Br Med J. 1960;2(5214):1708.
7) Hoang A, Nguyen T. Identifying Spatio-Temporal Clustering of the COVID-19 Patterns Using Spatial Statistics: Case Studies of Four Waves in Vietnam. Int J Appl Geospatial Res. 2022;13(1):1–15.
8) Kieu Q-L, Nguyen T-T, Hoang A-H. GIS and remote sensing: a review of applications to the study of the COVID-19 pandemic. Geogr Environ Sustain. 2021;14(4).
9) Gonzalez-Rubio J, Najera A, Arribas E. Comprehensive personal RF-EMF exposure map and its potential use in epidemiological studies. Environ Res. 2016;149:105–12.
10) Fecht D, Hansell AL, Morley D, Dajnak D, Vienneau D, Beevers S, et al. Spatial and temporal associations of road traffic noise and air pollution in London: Implications for epidemiological studies. Environ Int. 2016;88:235–42.
11) Alves JD, Abade AS, Peres WP, Borges JE, Santos SM, Scholze AR. Impact of COVID-19 on the indigenous population of Brazil: A geo-epidemiological study. Epidemiol Infect. 2021;149:e185.
12) Şener R, Türk T. Spatiotemporal analysis of cardiovascular disease mortality with geographical information systems. Appl Spat Anal Policy. 2021;14(4):929–45.
13) Xie Z, Qin Y, Li Y, Shen W, Zheng Z, Liu S. Spatial and temporal differentiation of COVID-19 epidemic spread in mainland China and its influencing factors. Sci Total Environ. 2020;744:140929.
14) Aral N, Bakır H. Spatiotemporal pattern of Covid-19 outbreak in Turkey. GeoJournal. 2023;88(2):1305–16.
15) Zhang P, Yang S, Dai S, Aik DHJ, Yang S, Jia P. Global spreading of Omicron variant of COVID-19. Geospat Health. 2022;17(s1).
16) Nguyen HX, Chu C, Nguyen HLT, Nguyen HT, Do CM, Rutherford S, et al. Temporal and spatial analysis of hand, foot, and mouth disease in relation to climate factors: a study in the Mekong Delta region, Vietnam. Sci Total Environ. 2017;581:766–72.
17) Deng T, Huang Y, Yu S, Gu J, Huang C, Xiao G, et al. Spatial-temporal clusters and risk factors of hand, foot, and mouth disease at the district level in Guangdong Province, China. PLoS One. 2013;8(2):e56943.
18) Shariati M, Mesgari T, Kasraee M, Jahangiri-Rad M. Spatiotemporal analysis and hotspots detection of COVID-19 using geographic information system (March and April, 2020). J Environ Heal Sci Eng. 2020;18:1499–507.
19) Al-Kindi KM, Alkharusi A, Alshukaili D, Al Nasiri N, Al-Awadhi T, Charabi Y, et al. Spatiotemporal assessment of COVID-19 spread over Oman using GIS techniques. Earth Syst Environ. 2020;4:797–811.
20) Samphutthanon R, Kumar Tripathi N, Ninsawat S, Duboz R. Spatio-temporal distribution and hotspots of hand, foot and mouth disease (HFMD) in northern Thailand. Int J Environ Res Public Health. 2014;11(1):312–36.

21) Xiao G, Hu Y, Ma JQ, Hao YT, Wang XF, Zhang YJ, et al. Spatial clustering and changing trend of hand-foot-mouth disease during 2008-2011 in China. Zhonghua liu xing bing xue za zhi= Zhonghua liuxingbingxue zazhi. 2012;33(8):808–12.
22) Ooi CH, Kiyu A, Brooke G. Application of Geographical information System (GIS) in Outbreak of Hand, Foot and Mouth Disease (HFMD) in Sarawak. Int J Infect Dis. 2008;12:e188.
23) Sham NM, Krishnarajah I, Ibrahim NA, Lye M-S. Temporal and spatial mapping of hand, foot and mouth disease in Sarawak, Malaysia. Geospat Health. 2014;8(2):503–7.
24) Noraishah MS, Krishnarajah I. Use of GIS mapping for HFMD cases in Sarawak, Malaysia. Int J. 2016;5(10):1937–45.
25) VietNamNews. HCM City faces burden of hand, foot, mouth disease and dengue fever [Internet]. Available from: https://vietnamnews.vn/society/1551273/hcm-city-faces-burden-of-hand-foot-mouth-disease-and-dengue-fever.html
26) Thanh TC. Effects OF climate variations ON hand-foot-mouth disease IN HO CHI minh city. Vietnam J Sci Technol. 2016;54(2A):120.
27) Cliff AD, Ord JK. Spatial processes: models & applications. (No Title). 1981;
28) Getis A, Ord JK. Local spatial statistics: An overview. Spatial analysis: Modeling in a GIS environment. Longley, P., and M. Batty. Wiley, New York; 1996.
29) Vu D-T, Nguyen T-T, Hoang A-H. Spatial clustering analysis of the COVID-19 pandemic: A case study of the fourth wave in Vietnam. Geogr Environ Sustain. 2021;14(4).
30) Nguyen TT, Vu TD. Identification of multivariate geochemical anomalies using spatial autocorrelation analysis and robust statistics. Ore Geol Rev. 2019;111.
31) Anselin L. Local indicators of spatial association—LISA. Geogr Anal. 1995;27(2):93–115.
32) Anselin L, Syabri I, Kho Y. GeoDa: an introduction to spatial data analysis. In: Handbook of applied spatial analysis: Software tools, methods and applications. Springer; 2009. p. 73–89.